The Role of Plasma Membrane Intrinsic Protein Aquaporins in Water Transport through Roots: Diurnal and Drought Stress Responses Reveal Different Strategies between Isohydric and Anisohydric Cultivars of Grapevine[1][OA]

Rebecca K. Vandeleur, Gwenda Mayo, Megan C. Shelden[2], Matthew Gilliham, Brent N. Kaiser, and Stephen D. Tyerman*

School of Agriculture, Food, and Wine, University of Adelaide, Waite Campus, Urrbrae, South Australia 5064, Australia (R.K.V., M.C.S., M.G., B.N.K., S.D.T.); and Australian Centre for Plant Functional Genomics, School of Agriculture, Food, and Wine, University of Adelaide, Waite Campus, Urrbrae, South Australia 5064, Australia (G.M.)

We report physiological and anatomical characteristics of water transport across roots grown in soil of two cultivars of grapevine (*Vitis vinifera*) differing in response to water stress (Grenache, isohydric; Chardonnay, anisohydric). Both cultivars have similar root hydraulic conductances (L_o; normalized to root dry weight) that change diurnally. There is a positive correlation between L_o and transpiration. Under water stress, both cultivars have reduced minimum daily L_o (predawn) attributed to the development of apoplastic barriers. Water-stressed and well-watered Chardonnay had the same diurnal change in amplitude of L_o, while water-stressed Grenache showed a reduction in daily amplitude compared with well-watered plants. Hydraulic conductivity of root cortex cells (L_{pcell}) doubles in Chardonnay but remains unchanged in Grenache. Of the two most highly expressed plasma membrane intrinsic protein (PIP) aquaporins in roots (VvPIP1;1 and VvPIP2;2), only VvPIP2;2 functions as a water channel in *Xenopus laevis* oocytes. VvPIP1;1 interacts with VvPIP2;2 to induce 3-fold higher water permeability. These two aquaporins are colocated in the root from in situ hybridization and immunolocalization of VvPIP1 and VvPIP2 subfamily members. They occur in root tip, exodermis, root cortex (detected up to 30 mm), and stele. *VvPIP2;2* mRNA does not change diurnally or with water stress, in contrast to *VvPIP1;1*, in which expression reflects the differences in L_o and L_{pcell} between cultivars in their responses to water stress and rewatering. VvPIP1;1 may regulate water transport across roots such that transpirational demand is matched by root water transport capacity. This occurs on a diurnal basis and in response to water stress that corresponds to the difference in drought tolerance between the cultivars.

Root hydraulic conductance is usually lowest within the liquid component of the soil-plant-air continuum. The hydraulic conductance of roots can be highly variable in both time and space, which will affect soil-water extraction and shoot water status (Steudle and Peterson, 1998; Steudle, 2000a, 2000b). Steudle (2000a,

2000b) explains variation in root hydraulic conductivity (L_p; hydraulic conductance normalized to root surface area) in terms of the composite transport model based on the composite anatomical structure of roots, where water can move radially toward the xylem along three pathways: the apoplastic, symplastic, and transcellular. The symplastic and transcellular pathways are difficult to separate experimentally and are collectively considered as the cell-to-cell pathway (Steudle, 2000b). The extent to which water flow predominates in either pathway varies according to the relative hydraulic conductances of the pathways and the relative magnitude of hydrostatic versus osmotic gradients (Steudle, 2000a; Bramley et al., 2007b). Apoplastic flow can be altered irreversibly by anatomical changes, including Casparian bands and suberin lamellae (Steudle and Peterson, 1998). The conductance of the cell-to-cell pathway can be largely determined by the activity of aquaporins within the series array of membranes, which results in changes in conductance that can be relatively rapid and revers-

ible. An example is the rapid reduction in the hydraulic conductance of Arabidopsis (*Arabidopsis thaliana*) roots to anoxia, which is considered to be caused by the inhibition of plasma membrane aquaporins due to reduced cytoplasmic pH (Tournaire-Roux et al., 2003; Alleva et al., 2006).

Aquaporins are members of the major (membrane) intrinsic protein (MIP) family. They are highly hydrophobic proteins with six membrane-spanning domains and molecular masses of 26 to 34 kD. In the genomic sequence of Arabidopsis, 35 aquaporins have been identified (Johanson et al., 2001), while 28 are evident in the *Vitis* genome (Fouquet et al., 2008). The proteins are divided into four subfamilies: plasma membrane intrinsic proteins (PIPs), tonoplast intrinsic proteins (TIPs), NOD26-like intrinsic proteins, and small basic intrinsic proteins. The PIPs are further divided into two subclasses. In general PIP1s have little or no water channel activity in vitro, whereas the PIP2s show high water permeability when expressed in *Xenopus laevis* oocytes (Chaumont et al., 2000). Water permeability of aquaporins can be regulated by cytosolic pH and pCa (Gerbeau et al., 2002; Alleva et al., 2006), phosphorylation (Maurel et al., 1995; Johansson et al., 1998), large pressure pulses (Wan et al., 2004), and osmotic solutes (Ye et al., 2004; Vandeleur et al., 2005). It has been demonstrated that PIP1 and PIP2 members may interact either within the membrane or by targeting to the plasma membrane (Fetter et al., 2004; Zelazny et al., 2007).

Root L_p has been shown to vary diurnally in *Lotus japonicus* and sunflower (*Helianthus annuus*; Henzler et al., 1999; Tsuda and Tyree, 2000). Diurnal regulation of L_p has been associated with aquaporin gene expression (Henzler et al., 1999; McElrone et al., 2007). There can be a delay between changes in expression and subsequent changes in hydraulic conductivity (Lopez et al., 2003). Yamada et al. (1997) detected diurnal variation in *MIP* expression in the leaves of *Nicotiana excelsior*, while diurnal regulation was also observed in the permeability of motor cell protoplasts in relation to aquaporin *SsAQP2* expression of *Samanea saman* (Moshelion et al., 2002).

Root L_p is usually reduced when soil dries (North and Nobel, 1991, 1996). During drying conditions, L_p of roots of *Agave deserti* declined, partly because of the collapse of cortical cells, increased suberization, and embolism in xylem vessels (North and Nobel, 1991). Roots also shrink as a result of cortical cell collapse, which reduces contact between soil and roots. Use of mercuric chloride has demonstrated down-regulation of aquaporins in water-stressed desert plants and aspen (*Populus* spp.) seedlings (Martre et al., 2001; Siemens and Zwiazek, 2003; North et al., 2004). Gene expression studies in various plant species have shown variable responses of aquaporin isoforms to water stress, with both up- and down-regulation of genes evident (Yamada et al., 1997; Mariaux et al., 1998; Sarda et al., 1999; Suga et al., 2002; Jang et al., 2004; Alexandersson et al., 2005). In leaves, roots, and

twigs of olive (*Olea europaea*), *OePIP1;1*, *OePIP2;1*, and *OeTIP1;1* were significantly reduced at 3 and 4 weeks after water was withheld (Secchi et al., 2007). Overexpression of *AtPIP1b* in transgenic tobacco (*Nicotiana tabacum*) plants caused plants to wilt faster when water was withheld (Aharon et al., 2003). In contrast, Siefritz et al. (2002) observed reduced resistance to water stress in antisense tobacco plants with reduced expression of *NtAQP1*, the homologous aquaporin.

Grapevine (*Vitis vinifera*) has now become a model system for fruit trees (Troggio et al., 2008) based on the ease of clonal plant propagation and full genome sequence availability (Jaillon et al., 2007). There is also considerable phenotypic and genetic variation between cultivars of grapevine that are advantageous in comparative physiology and molecular studies (DeBolt et al., 2006; Tilbrook and Tyerman, 2008). Grapevine contributes substantially to economies, and in order to achieve high fruit quality and efficient water use, deficit irrigation techniques are commonly used. These result in various degrees of water stress, with roots exposed to cycles of drying and wetting over time scales ranging from diurnal to several days or weeks (Dry and Loveys, 1998).

Here, we have undertaken a comparative study between the two cultivars Grenache and Chardonnay to determine to what extent the cell-to-cell pathway and aquaporins affect changes to root hydraulic conductance in response to time of day and water stress. We expected changes in aquaporin expression to match changes in whole root and cell hydraulic conductivity in a genotype- × environment-dependent manner, broadly reflecting the different strategies to drought stress in the two cultivars. Grenache has been shown to be nearly isohydric, exerting a tight regulation of stomatal aperture that may contribute to drought tolerance (Schultz, 2003; Soar et al., 2006), and is considered to be more drought tolerant than Chardonnay (Alsina et al., 2007). Gibberd et al. (2001) presented data for transpiration efficiency and transpiration per unit leaf area for a number of cultivars, including Grenache and Chardonnay, grown in the same well-watered glasshouse conditions. Grenache had a much lower transpiration rate per unit leaf area than Chardonnay and shared similar characteristics of transpiration efficiency to that of some *Vitis* hybrids that are known to be drought tolerant.

We examined root hydraulic conductance (L_o; normalized to root dry weight) induced by water stress, taking into account variation that may be linked to transpiration rate of the shoots, to see if changes in L_o were consistent with the observed changes in root apoplastic barriers, cortical cell hydraulic conductivity, and the mRNA expression of PIP aquaporins. We functionally characterized the two most highly expressed PIP aquaporins in the root (*VvPIP1;1* and *VvPIP2;2*) by expression in *Xenopus* oocytes to determine whether they interact, and we examined the sites of expression and protein location in the root for evidence of colocation.

RESULTS

Variation in Hydraulic Conductance of Whole Root Systems

There was a large degree of variation in the root L_o (normalized to root dry weight) of well-watered grapevine between experiments (different batches of plants grown at different times) and during a single day within a batch of plants grown under the same conditions. During a 24-h period, L_o of well-watered Chardonnay vines was measured five times; it varied diurnally, peaking in the middle of the day before declining during the evening (Fig. 1A). By combining L_o values of well-watered Chardonnay and Grenache plants from all experiments described in this paper, a positive relationship was observed between transpiration rate (E) measured before plants were harvested and root L_o (Fig. 1B). There was no significant difference between cultivars in the regressions of L_o versus transpiration rate; the regression line for the combined data is shown in Figure 1B. Grenache also showed a similar diurnal variation under well-watered conditions (Fig. 2).

Impact of Water Stress on Diurnal Variation

Compared with well-watered conditions, Chardonnay root systems in response to water stress had an almost 2-fold reduction in L_o at 2:00 PM and a 4-fold reduction prior to sunrise (6:00 AM; Fig. 2). In contrast, water-stressed Grenache maintained a 4.5-fold lower L_o at both 6:00 AM and 2:00 PM compared with the well-watered controls (Fig. 2). The similar magnitude of diurnal amplitude of L_o of water-stressed Chardonnay roots compared with the controls between 6:00 AM and 2:00 PM contrasts with a large decrease in amplitude of diurnal variation in L_o for water-stressed Grenache root systems over the same period (Fig. 2). Although

the stem water potential (Ψ_{stem}) at midday was slightly lower in Grenache than in Chardonnay under water stress in this experiment, subsequent experiments confirmed that Grenache consistently gave a larger reduction in L_o for similar reductions in Ψ_{stem}, independent of growth conditions. With the two-pot system, there was a 5.5-fold reduction in L_o under water stress compared with a 5.5-fold reduction in a single-pot experiment under the same growth conditions.

Response to Subsequent Rewatering after Water Stress

The effects of water stress and subsequent rewatering were investigated in another set of experiments. This was done in separate experiments for each cultivar to allow measurements of root L_o over a sufficiently narrow range of time in the middle of the day. Control values of root L_o for Grenache (1.43×10^{-6} kg s^{-1} MPa^{-1} g^{-1}) were similar to those shown in Figure 2, but Chardonnay in this case had almost twice the value of root L_o (2.90×10^{-6} kg s^{-1} MPa^{-1} g^{-1}), corresponding to higher transpiration rates in this particular experiment (data included in Fig. 1B). Chardonnay gave a 3.2-fold reduction in L_o when water stressed, but Grenache showed a much larger 6.5-fold reduction, consistent with the findings reported in Figure 2. There was no correlation between the extent of the reduction in L_o and the extent to which midday Ψ_{stem} was reduced ($r^2 = 0.592$, $P > 0.05$) at least for the range of midday Ψ_{stem} achieved under water stress.

One day after rewatering, there was no significant increase in L_o above the value for water-stressed Chardonnay vines (fold difference between controls and drought and rewatered = 2.9). L_o of Grenache did show some recovery (fold difference between controls and drought and rewatered = 3.3), but the increase was not significant.
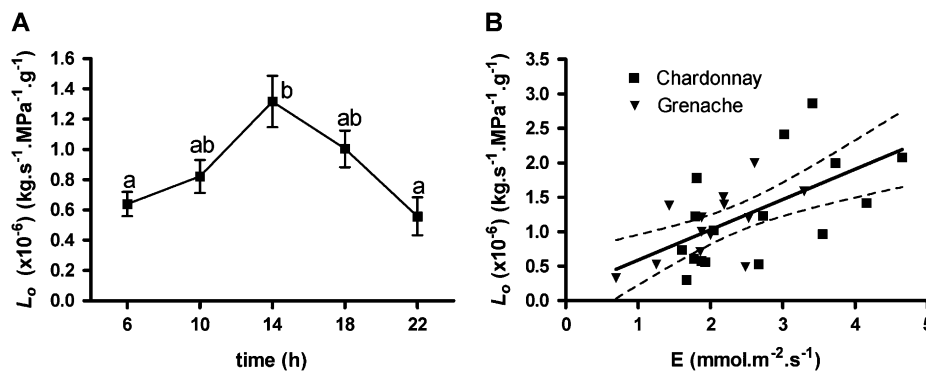

Figure 1. Variation in L_o normalized to root dry weight. A, Diurnal change in L_o of well-watered Chardonnay plants within a 24-h period. Values are means ± SE of four plants. Different letters indicate values that are significantly different (Tukey's test, $P <$ 0.05). B, L_o measured between 1:00 and 3:00 PM plotted against average transpiration rate (E) measured between 11:00 AM and 12:00 noon. The equation for the linear regression is $L_o = m \times E + b$, where $m = 0.47$ and $b = 0.03$ ($r^2 = 0.369$) for Chardonnay and $m = 0.45$ and $b = 0.18$ ($r^2 = 0.381$) for Grenache. Regressions for the two cultivars were not significantly different; thus, the combined regression, with 95% confidence levels, is shown.
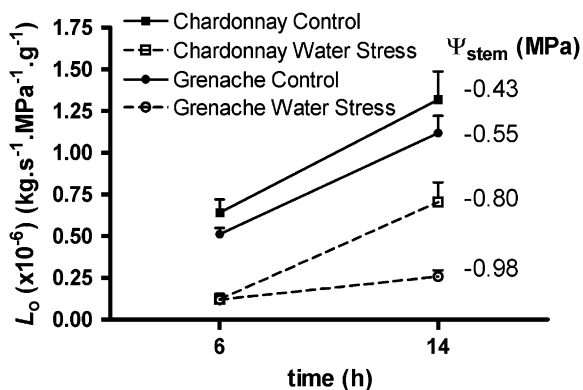
Figure 2. Effect of water stress on the change in amplitude of L_o between 6:00 AM and 2:00 PM. Diurnal change in L_o is shown for both cultivars under well-watered and water-stressed conditions. Ψ_{stem}, measured between 11:00 AM and 1:00 PM on the day of harvest, for L_o is indicated to the right of the associated points. The Chardonnay and Grenache plants were from different experiments. Values are means ± SE of four plants. Within each cultivar, the effects of time of measurement and water stress treatment were significant (two-way ANOVA, $P < 0.05$; the interaction was significant only for Grenache).

Cortical Cell Water Relations

In order to examine how cortical cell hydraulic conductivity (L_{pcell}) responds to water stress and to examine differences between the cultivars, pressure probe experiments were performed. Plants were water stressed in the same manner as above and to similar Ψ_{stem}. The midday Ψ_{stem} of water-stressed Chardonnay used for cell pressure probe measurements and root anatomy (see below) decreased from −0.50 to −1.15 MPa, while Grenache Ψ_{stem} decreased from −0.55 to −1.20 MPa. Roots were harvested from a basal pot (see "Materials and Methods") and bathed in 1 mM $CaSO_4$ to perform pressure probe measurements on root cortical cells 25 to 30 mm from the root apex. Steady turgor pressures recorded in cortex cells under these conditions ranged from very low values for roots from water-stressed plants (sometimes less than 0.08 MPa) up to 0.5 MPa for roots harvested from control plants (Table I). Both varieties showed a significant positive relationship between $\Delta P/\Delta V$ and turgor pressure that was due to a turgor-dependent volumetric elastic modulus ($\varepsilon = mP + b$, where $m = 13.16 \pm 1.303$ and $b = 0.6787 \pm 0.2860$ MPa; $r^2 = 0.98$). This was not significantly different between the two cultivars.

The data in Table I summarize cell dimensions of cortical cells that were used to calculate L_{pcell}. For both cultivars, cell dimensions were significantly altered in response to water stress. Both Grenache and Chardonnay had similar cell radii and showed reductions in radius under water stress, but in contrast to Chardonnay, Grenache had a substantially increased cell length under water stress.

L_{pcell} increased in response to water stress in Chardonnay roots (Fig. 3), as indicated by a significant decrease in relaxation half-times (Table I). The increase

in L_{pcell} observed for Grenache roots (Fig. 3) was not significant, and there was a lack of impact of water stress on relaxation half-times (Table I).

Changes in Suberin Deposition in Response to Water Stress

Qualitative changes in suberin lamellae deposition in the roots in response to water stress were examined at 50 mm from the root tip. The Ψ_{stem} values at midday of the plants used were the same as those used for cortical cell water relations. In the cell layer beneath the epidermis that contains Casparian bands (exodermis, Fig. 4, A–D), there was a greater intensity of suberin deposited in cell walls of water-stressed roots than in well-watered roots for both cultivars (Chardonnay [Fig. 4, C and D], Grenache [Fig. 4, A and B]). Exodermal cells of water-stressed roots of both cultivars had suberin lamellae deposited on the outer tangential walls in addition to the radial and inner tangential walls observed in both treatments. Passage cells were still evident in the water-stressed roots of both cultivars.

In well-watered roots at 50 mm from the root tip, only a limited number of endodermal cells had suberin lamellae (Fig. 4, E and G). In some roots, there was deposition of suberin lamellae, but passage cells still remained, aligned with the xylem poles. Water-stressed roots appeared to have more endodermal cells with suberin lamellae (Fig. 4, F and H). In the case of Chardonnay, passage cells were generally still evident (Fig. 4H), but in Grenache, all cells of the endodermis appeared to have become suberized (Fig. 4F).

Gene Expression of PIP Aquaporins

Five *VvPIP1* members and four *VvPIP2* members of the PIP aquaporin subfamily were identified as full-length sequences from the sequenced genome of grapevine (Jaillon et al., 2007). Recently, eight members of the PIP subfamily were identified from the sequenced genome (Fouquet et al., 2008). Screening of a cDNA library constructed from Cabernet Sauvignon vegetative tissue resulted in the identification of six PIP1 aquaporins and five PIP2 aquaporins (Shelden, 2007). Of these, *VvPIP1;1* and *VvPIP2;2* were the most highly expressed relative to grapevine actin transcript (*VvACT1*) in roots sampled at midday of well-watered Chardonnay plants (Fig. 5). A similar result was found for Grenache roots (results not shown). The responses of these two aquaporins diurnally and to water stress were examined in more detail. *VvPIP2;2* appeared to be constitutively expressed irrespective of time or treatment, with only slight changes in the level of expression relative to *VvACT1* (Fig. 6, A and B), but relative expression of *VvPIP1;1* changed significantly (Fig. 6, A and C). Diurnally, *VvPIP1;1* expression levels peaked at 10:00 AM in Chardonnay roots, and a similar expression level was maintained while the lights were on and then was significantly reduced during the dark

Table I. *Cell size and water relation parameters of root cortical cells of well-watered and water-stressed Chardonnay and Grenache*

Measurements were made in the third or fourth layer of cortical cells, 25 to 30 mm from the root tip. Values with different letters within a row are significantly different ($P < 0.05$).

Parameter	Chardonnay		Grenache	
	Control	Water Stressed	Control	Water Stressed
Cell radius[a] (μm)	26.9 $\pm$ 1.2 a (36)	21.4 $\pm$ 0.9 b,c (45)	24.3 $\pm$ 0.9 a,b (79)	19.9 $\pm$ 0.8 c (90)
Cell length[b] (μm)	106.0 $\pm$ 4.1 a (65)	105.0 $\pm$ 3.0 a (69)	111.8 $\pm$ 4.9 a (35)	142.6 $\pm$ 3.9 b (55)
Water relations	$n = 18$	$n = 19$	$n = 18$	$n = 21$
$T_{1/2}$ (s)	1.68 $\pm$ 0.16 a	0.96 $\pm$ 0.12 b	1.11 $\pm$ 0.13 b	1.12 $\pm$ 0.14 b
ε (MPa)	4.45 $\pm$ 0.70 a	1.54 $\pm$ 0.10 b	4.65 $\pm$ 0.25 a	2.34 $\pm$ 0.18 c
π_l (MPa)	0.30 $\pm$ 0.02 a	0.08 $\pm$ 0.01 b	0.29 $\pm$ 0.02 a	0.11 $\pm$ 0.03 b

[a]Cells of six roots from three plants were measured; total number of cells measured is shown in parentheses. [b]Cells of four roots from two plants were measured; total number of cells measured in shown in parentheses.

period (Fig. 6A). Grenache and Chardonnay differed in *VvPIP1;1* expression response to water stress and rewatering, with similar changes in Ψ_{stem}. In this experiment, midday Ψ_{stem} of water-stressed Chardonnay decreased from -0.30 to -0.90 MPa and increased to -0.30 MPa at 24 h after rewatering. Grenache Ψ_{stem} decreased from -0.35 to -0.90 MPa and increased to -0.35 MPa. *VvPIP1;1* showed an approximately 3-fold increase in level of expression in response to water stress in the roots of Chardonnay (Fig. 6C). This declined to the level of the control plants upon rewatering. In contrast to Chardonnay, Grenache did not show a significant increase in *VvPIP1;1* expression due to water stress (Fig. 6C), and transcript level was significantly higher in rewatered roots compared with control roots (Fig. 6C). The L_o of Grenache roots was measured in the double-pot configuration for this experiment. There was an approximately 5-fold reduction in L_o in response to water stress and a slight but nonsignificant recovery at 24 h after rewatering. This result was similar to that observed in the single-pot experiments described above.

Water Channel Activity of VvPIP1;1 and VvPIP2;2

Water transport activity of VvPIP1;1 and VvPIP2;2 was examined in *Xenopus* oocytes. Data shown in Figure 7 are the combined results of two separate experiments, each with five oocytes. Osmotic water permeability (P_{os}) was calculated from the rate of increase in the volume of oocytes when exposed to a hypotonic solution. The P_{os} of oocytes expressing *VvPIP1;1* was not significantly greater than that of oocytes injected with water (Fig. 7). Oocytes injected with *VvPIP2;2* had a P_{os} 2-fold larger than oocytes expressing *VvPIP1;1*. When *VvPIP1;1* and *VvPIP2;2* cRNA were injected together, there was a 3-fold increase in P_{os} above the level of *VvPIP2;2* alone. Varying the amount of *VvPIP1;1* (6–36 ng) injected with

VvPIP2;2 (12 ng) did not significantly alter this increase in P_{os}.

Location of VvPIP1;1 and VvPIP2;2 in Roots

Figure 8 shows in situ hybridization of *VvPIP2;2* and *VvPIP1;1* antisense and sense (control) probes for both cultivars. All sense probe controls showed minimal background hybridization, so for the sake of brevity, images were only included for one gene per cultivar. Controls made with no probe showed no signal in any tissues and, therefore, are not presented. Grenache and Chardonnay roots displayed similar localized patterns of *VvPIP1;1* and *VvPIP2;2* mRNA expression. For both genes, strong signal was detected in elongating cortical tissue and vascular tissue of root tip longitudinal sections, with the strongest signal in the root apex (Fig. 8). At 30 and 50 mm from the root apex, transverse
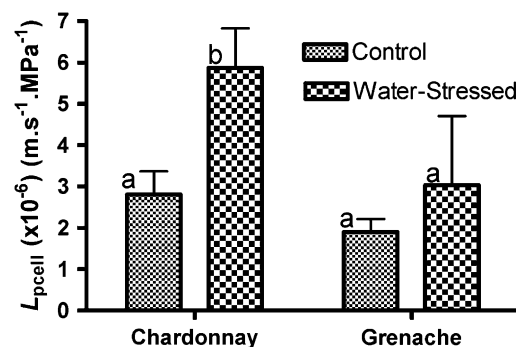
Figure 3. L_{pcell} of third- and fourth-layer cortical cells of Chardonnay and Grenache roots. L_{pcell} for both cultivars is shown for control and water-stress treatments. Measurements were taken 25 to 30 mm from the root tip. Values are means $\pm$ SE (calculated for error propagation of component measured variables) of 18 to 23 cells. Different letters indicate values that are significantly different within a cultivar (*t* test, $P < 0.05$).
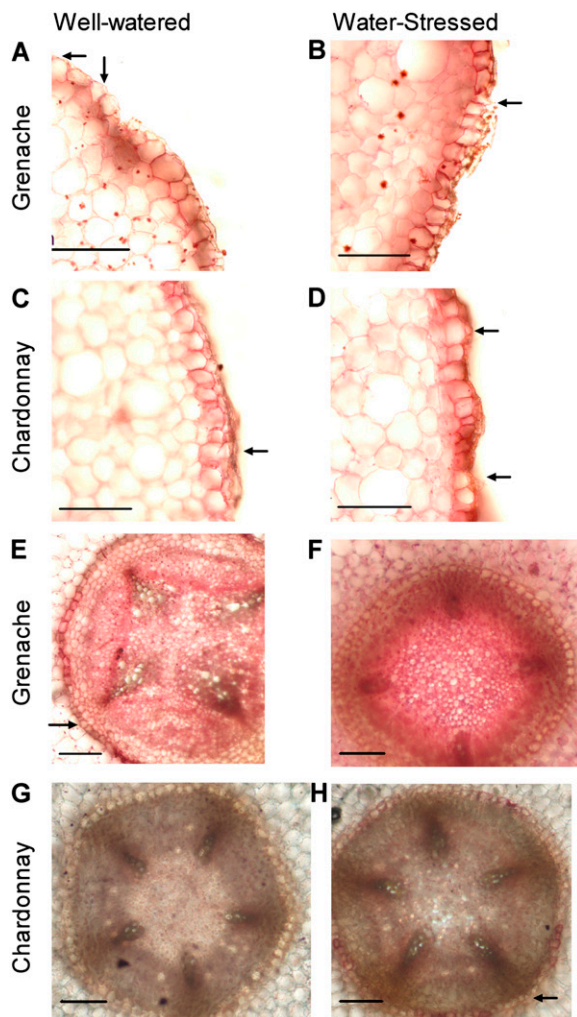
Figure 4. Root suberin lamellae. Cross sections of Grenache (A, B, E, and F) and Chardonnay (C, D, G, and H) roots taken 50 mm from the root tip and stained with Sudan Red 7B for 2 h to show suberin lamellae. Roots from well-watered plants are on the left, and roots from water-stressed plants are on the right. The exodermis (A–D) and endodermis (E–H) are shown. Examples of passage cells are indicated by the arrows. Bars = 100 μm.

sections revealed that *VvPIP2;2* expression occurred in vascular tissue adjacent to and between the xylem poles and also in the cortex. Expression of *VvPIP1;1* at 30 and 50 mm from the root apex was not consistently detected. The brown material evident in the root, in particular in the epidermis and endodermis, is likely to be phenolic compounds.

To examine the general patterns of protein expression of VvPIP2 and VvPIP1 subgroups, antibodies were raised to peptides designed to detect grapevine PIP1 or PIP2 members based on the conserved N and C termini that differ between the two subgroups (Schäffner, 1998). Longitudinal sections showed signal throughout the elongation zone and in the cortical tissue and vascular tissue for both antibodies (Fig. 9). At 30 and 50 mm from the root tip, strong VvPIP1

signal was detected in the vascular tissue and exodermis, with reduced signal in the cortex (Fig. 9). VvPIP2 signal pattern was similar to VvPIP1 but weaker and was more consistently seen in the vascular tissue and exodermis than in the cortex (Fig. 9). There was a strong signal for both groups of proteins in cells closely associated with xylem vessels and phloem cells. Controls with no primary and secondary antibodies revealed the background autofluorescence of grapevine root tissues (Fig. 9). Controls with a single antibody (no primary or no secondary) did not differ from the latter controls.

DISCUSSION

Changes in Root Hydraulic Conductance

Root L_o of both Chardonnay and Grenache grapevine under well-watered conditions showed considerable variation in the various experiments described in this study. This variation may be linked to differences in transpiration from one experiment to another and to diurnal variation associated with changes in transpiration rate during the day, which is partly dependent on light intensity.

At low water flow (low transpiration), the composite transport model predicts some circulation flow of water across the root, because osmotic gradients may become more significant and there should be a large difference in the reflection coefficients for the cell-to-cell and apoplastic pathways. It has been proposed that with increasing transpiration and xylem tension there will be an increase in root L_o, because a greater proportion of radial flow occurs via the apoplast pathway in response to increasing hydrostatic gradients (Steudle and Heydt, 1997). A positive relationship between apparent L_o and stomatal conductance has been shown previously (Meinzer and Grantz, 1990; Sperry et al., 1993; Saliendra et al., 1995). Modeling by
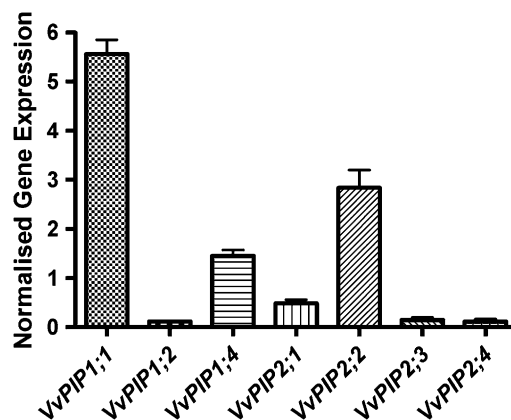

Figure 5. Relative gene expression of seven PIPs in well-watered Chardonnay roots. Values are means ± SE of two biological replicates sampled at midday. Relative gene expression was normalized to the expression of *VvACT1* according to the method of Muller et al. (2002).
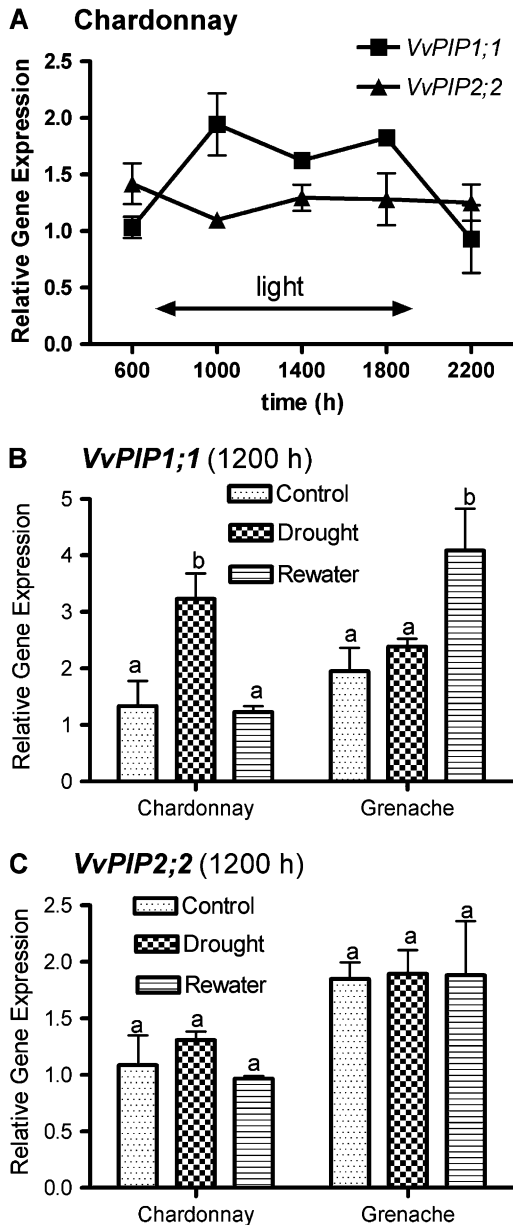
A Chardonnay

B VvPIP1;1 (1200 h)

C VvPIP2;2 (1200 h)

Figure 6. *VvPIP1;1* and *VvPIP2;2* gene expression. A, Relative gene expression of *VvPIP1;1* and *VvPIP2;2* in response to time of day for well-watered Chardonnay roots. Lights were on between 7:00 AM and 7:00 PM. Values are means ± SE of three biological replicates. B, Relative expression of *VvPIP1;1* in response to water stress and rewatering for Chardonnay and Grenache at 12:00 noon. C, Relative expression of *VvPIP2;2* in response to water stress and rewatering for Chardonnay and Grenache at 12:00 noon. Relative gene expression is the ratio of the starting quantity of the gene of interest and the starting quantity of *VvACT1*. Values are means ± SE of three biological replicates. For each cultivar, columns with different letters are significantly different ($P < 0.05$).

Franks et al. (2007) showed that a dependence of hydraulic conductance on transpiration rate would explain the responses they observed in leaf water potential of *Eucalyptus gomphocephala* in response to

changes in soil water. However, there is a crucial difference between most of these studies and our measurements. We measured L_o under identical pressure gradients and identical conditions for all experiments. Thus, the explanation for an increase in L_o based on the composite transport model, in which gradients are different, probably does not account for our observations. Solute polarization was not evident, because there was no change in conductance obtained from successive pressure ramps. The volume of fluid injected into the root was also small relative to the total root volume. Therefore, we conclude from our measurements that the variation in L_o is a function of intrinsic changes to permeability barriers in the roots, which are affected by the conditions that the plants were under at the time of harvest. These changes appear to persist for at least the time that it takes to decapitate the shoot and take the root systems into the laboratory for measurement with the hydraulic conductance flow meter.

Grapevine, along with a number of other plant species, demonstrates a reduction in root hydraulic conductivity in response to water stress. This has been intensively investigated in desert plants (North and Nobel, 1995, 1996, 2000; Martre et al., 2001; North et al., 2004). In some of these cases, reduction was associated with a closure of aquaporins, as evidenced by the inability of mercuric chloride to further reduce hydraulic conductivity under water-stressed conditions (Martre et al., 2001; North et al., 2004). This was suggested as a mechanism to prevent water loss to the soil, which has a lower water potential than the plant. Similar results were seen for severely stressed aspen seedlings (Siemens and Zwiazek, 2003).

This study discovered a remarkable difference in diurnal change in L_o between the two cultivars in response to water stress (Fig. 2). A reasonable assumption is that relatively rapid (daily) and reversible changes in L_o can only occur via changes in cell membrane water permeability, probably via aquaporins, as we discuss below. In Grenache, the apparent scale of the change in L_o would suggest that the same relative changes in cell membrane permeability occur over a diurnal period but that much less root surface area (or dry weight) is able to conduct water under water stress. Under water stress, Chardonnay showed a similar reduction in predawn L_o as Grenache but a smaller reduction in midday L_o, indicating that cell membrane water permeability increased to a much larger extent between predawn and midday under water stress.

One day after rewatering, neither cultivar showed a significant increase in L_o. An increase in L_o following rewatering may be delayed while significant changes in root anatomy are overcome by new lateral roots and the resumption of apical root growth. *Olea oleaster* appeared to recover only after 48 to 72 h of rewatering, when new lateral roots had emerged and root tips resumed growth (Lo Gullo et al., 1998). In contrast to our results with grapevine, there were significant

Figure 7. Functional expression of *VvPIP1;1* and *VvPIP2;2* in *Xenopus* oocytes. P_{os} of oocytes was measured from swelling kinetics. Oocytes were injected with 46 nL of cRNA solution or water. The quantities of *VvPIP1;1* and *VvPIP2;2* cRNAs used are shown on the left. Values are means of measurements of 10 oocytes ± SE. Columns with different letters are significantly different ($P < 0.05$).
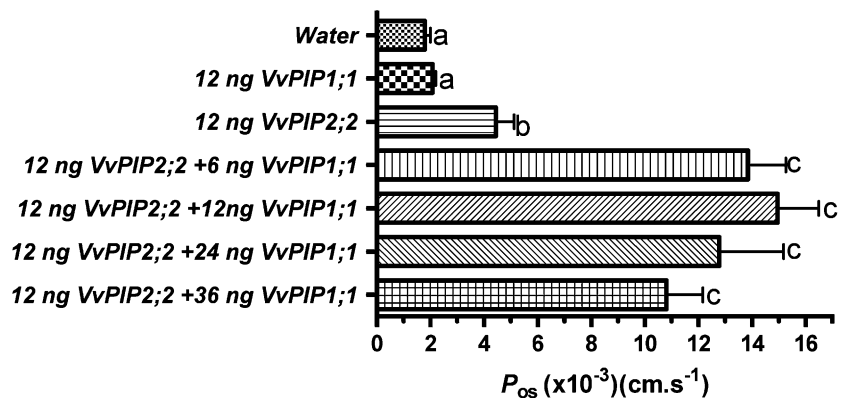
increases in hydraulic conductivity when desert plants were rewatered (North et al., 2004). This is likely to be an adaptation to the environmental conditions with limited rainfall events in which desert plants grow.

Suberization increased in the roots of both cultivars as a consequence of water stress. Passage cells remained in the endodermis of Chardonnay, whereas the endodermis was completely suberized 50 mm from the root tip of Grenache. The association between increased suberization in the roots and reduced hydraulic conductivity has been observed previously in *A. deserti* (North and Nobel, 1991) and sorghum (*Sorghum bicolor*; Cruz et al., 1992). The increased suberization under water stress for both cultivars of grapevine probably accounts for the reduced "baseline" L_o measured at predawn.

Changes in Cortical Cell Water Relations

From a comparison of diurnal changes in L_o under water-replete and water-stressed conditions, it was expected that Chardonnay would have increased cell-to-cell conductance to water under water stress at midday compared with Grenache. We observed a significant increase in L_{pcell} of water-stressed Chardonnay cortical cells and no significant change in L_{pcell} of water-stressed Grenache roots. These results indicate clear cultivar differences that are in line with the proportional changes in the diurnal amplitude of root L_o under water stress. These changes also correlate with the different pattern of expression of *VvPIP1;1* between cultivars in response to water stress discussed below. These measurements were obtained for roots growing into a different medium than the majority of roots in the two-pot system. Therefore, we cannot exclude the possibility that the roots in the bottom pot may behave differently from the majority of the root system in the top pot. However, given that there was no difference in response of root L_o between one-pot and two-pot cultivation, and given the correlations between whole root system L_o and *VvPIP1;1* expression and cell L_p, we think that an entirely different qualitative behavior between sampled roots and the whole root system is unlikely.

The reduced cortical turgor pressure seen in water-stressed roots was not expected. Assuming that cells had accumulated solutes for osmotic adjustment, it would be expected that water would rapidly move into cells once the root was placed in a solution of low osmotic pressure (necessary in our case to perform the measurements). This would cause turgor pressure to increase compared with that in control roots. Another possibility is that the osmotic concentration of the apoplast around the cortical cells is increased under water stress and that there is reduced exchange between the apoplast and the external medium because of the dermal apoplastic barriers. This may lead to a decrease in measured turgor even if the osmotic concentration in the cells is maintained or increased compared with that in controls. Using osmotic pressure of control roots for the calculation of L_{pcell} in water-stressed roots did not strongly affect the magnitude of the L_{pcell}.

There is minimal evidence of osmoregulation in grapevine roots in the literature. Düring and Dry (1995) observed osmoregulation in the apical 3 mm of grapevine roots (cv Kober 5BB). Osmoregulation was observed in other parts of the root, but only after a number of cycles of severe and rapid water stress. The work of Sharp and others with turgor regulation in root cells has concentrated on the apical 10 mm of maize (*Zea mays*) roots (Sharp et al., 1990, 2004; Voetberg and Sharp, 1991). At 25 mm from the root tip, the radius of cortical cells in water-stressed grapevine roots was reduced, which may suggest a loss of turgor, although cell extensibility will have an important role and is known to change under water stress (Wu et al., 1996; Fan et al., 2006). Therefore, it is possible that osmoregulation in grapevine roots occurs mostly in the root apices to enable root growth to recommence when the plants are rewatered or to maintain root elongation in drying soil.

Changes in Expression of *VvPIP1;1* and *VvPIP2;2*

Diurnal variation in L_o for Chardonnay root systems was associated with changes in the level of *VvPIP1;1*. However, *VvPIP2;2* appeared to be constitutively ex-
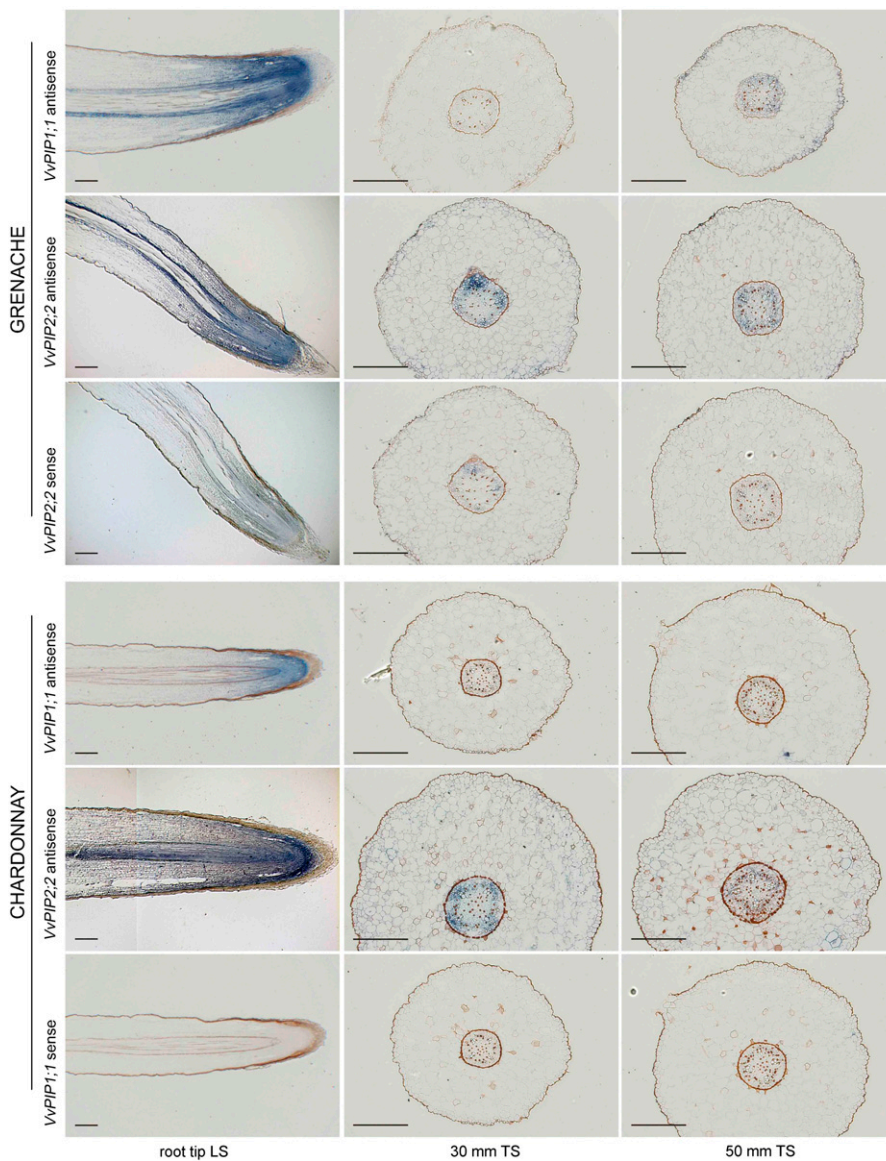
Figure 8. In situ localization of *VvPIP1;1* and *VvPIP2;2* mRNA in Grenache and Chardonnay roots. Blue signal indicates the location of antisense *VvPIP1;1* and *VvPIP2;2* probes on each grape cultivar. Sense probe controls are only presented for one gene per grape cultivar, to indicate background staining. Transverse sections (TS) were taken 30 and 50 mm from the root tip. LS, Longitudinal section. Bars = 250 μm.

pressed. In *L. japonicus*, the diurnal change in hydraulic conductivity of excised roots was associated with changes in the abundance of a putative *PIP1* aquaporin (Henzler et al., 1999). The highly variable response to water stress of aquaporins at the transcript level depends on species, type of water stress, degree of water stress, and the plant organ (Tyerman et al., 2002; Bramley et al., 2007a). Individual isoforms also vary in their response, all of which makes interpretation of the role of aquaporins during water stress rather difficult. However, in our case, the expression data do assist in the interpretation of the different responses of Grenache and Chardonnay to water stress.

The observation of similar diurnal changes in amplitude of Chardonnay L_o under water-stressed and well-watered conditions suggests that cell-to-cell conductance increased to a larger extent during the day under water stress. At one extreme, where most of the radial flow may occur through the cell-to-cell pathway, the fold changes possible for cell-to-cell conductance from predawn to midday are calculated to be from 2.5-fold under water-replete conditions to 6.6-fold under water stress. In Grenache, there was no indication that the diurnal change in cell-to-cell conductance would need to be different. This is supported by the increase in transcript level of *VvPIP1;1* in the roots of water-stressed Chardonnay vines at midday compared with no change in Grenache.

A number of researchers have previously observed the up-regulation of aquaporins in response to water stress in other plant species (Jang et al., 2004; Alexandersson et al., 2005; Aroca et al., 2006). The use of transgenic plants with overexpressing or underexpressing PIP1 also supports the importance of PIP1 for tolerance to water stress (Siefritz et al., 2002; Yu et al., 2005). Arabidopsis plants expressing *Vicia faba*

Figure 9. Immunolocalization of VvPIP1 and VvPIP2 proteins in Grenache and Chardonnay roots. VvPIP1 antibody is specific to all PIP1s, and VvPIP2 antibody is specific to all PIP2s. Controls with no primary or secondary antibody indicate cells with background autofluorescence. Transverse sections (TS) were taken 30 and 50 mm from the root tip. LS, Longitudinal section. Bars = 250 μm.
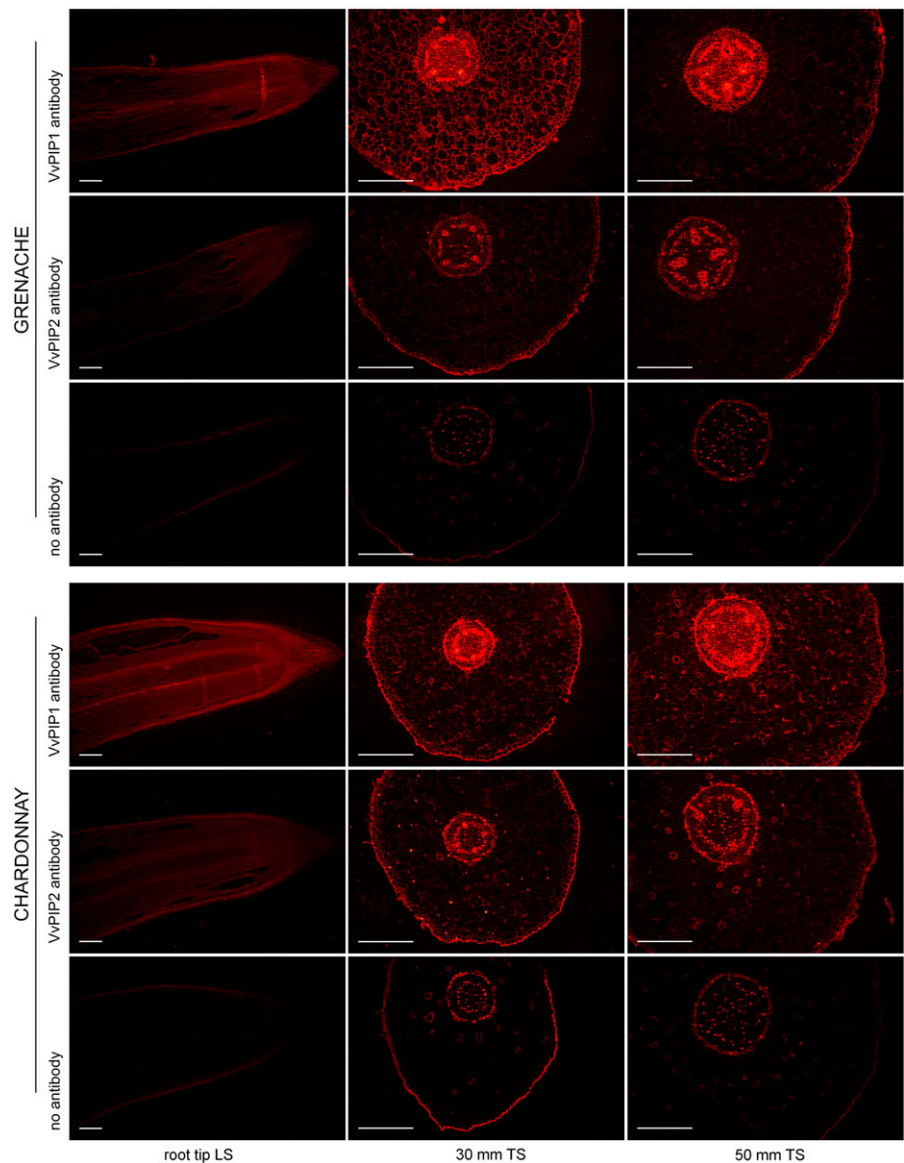
VfPIP1 had longer roots and a greater number of lateral roots, which may have contributed to improved drought resistance (Cui et al., 2008). Our results for Chardonnay support the view that increased aquaporin levels can be associated with adaptation to water stress. This contrasts with the strategy suggested for desert plants and aspen seedlings, in which aquaporins are down-regulated to prevent water loss to the soil (Martre et al., 2001; Siemens and Zwiazek, 2003; North et al., 2004).

The more drought-tolerant Grenache showed a different response to Chardonnay, with a reduction in diurnal change in root L_o due to water stress, indicating either a maintained or a reduced diurnal amplitude of cell-to-cell conductance. This was associated with a lack of change in transcript level of *VvPIP1;1* and *VvPIP2;2*. A similar result for homologs of the two

genes was observed by Galmés et al. (2007) in the roots of a drought-tolerant grapevine rootstock, Richter 110 (*Vitis berlandieri* $\times$ *Vitis rupestris*), with the exception that after 7 d at a soil water deficit there was an increase in *PIP2;2*. It is possible that other aquaporin isoforms not examined in our study were down-regulated or that there were posttranslational changes causing reductions in aquaporin activity. Grenache seems to have a more conservative approach in its response to drought stress, similar to the desert plants. A combination of anatomical changes and reduced aquaporin gene expression or activity is likely to be the cause of the much larger reduction in hydraulic conductivity at midday observed for Grenache.

When Grenache plants were rewatered, the slight recovery in L_o, although not significant, was associated with an up-regulation of *VvPIP1;1*. In the distal re-

gions of the desert plants *A. deserti* and *Opuntia acanthocarpa*, a significant recovery in hydraulic conductivity was associated with an increase in aquaporin activity, determined by the impact of mercuric chloride (Martre et al., 2001; North et al., 2004). Arabidopsis plants with reduced (antisense) expression of *PIP1* and *PIP2* aquaporins were slower to recover hydraulic conductance and transpiration rates at 4 d after rewatering (Martre et al., 2002).

As shown in a number of other plant species, VvPIP2;2 had much higher water permeability in oocytes than VvPIP1;1. Moshelion et al. (2002) observed that SsAQP1 (from the PIP1 group) had a permeability that was twice that of the control, but SsAQP2 (from the PIP2 group) was 10-fold higher again. ZmPIP1a and ZmPIP1b had no water channel activity in oocytes (Chaumont et al., 2000). Positive interaction between a PIP1 and PIP2 has been demonstrated in other plant species but is not always observed (Zhou et al., 2007). Fetter et al. (2004) and Temmei et al. (2005) both demonstrated interaction between aquaporins from the PIP1 subclass and the PIP2 subclass. In living maize cells, it appears that interaction is required to traffic PIP1 from the endoplasmic reticulum to the plasma membrane (Zelazny et al., 2007). In lily (*Lilium longifolium*) pollen, protoplast expression of Arabidopsis aquaporins AtPIP1;1 and AtPIP1;2 did not increase water permeability, in contrast to the increase observed with AtPIP2;1 and AtPIP2;2 (Sommer et al., 2008). Coexpression of AtPIP1;1 or AtPIP1;2 with AtPIP2;1 or AtPIP2;2 did not elevate protoplast water permeability above that when AtPIP2;1 or AtPIP2;2 was expressed alone. However, the authors did point out that a native PIP1 may have interacted with AtPIP2 to increase water permeability. Varied levels of VvPIP1;1 protein may influence the water permeability of the transcellular pathway across grapevine roots when interacting with VvPIP2;2. Our results with coexpression in *Xenopus* showed a positive interaction, but there was

no indication over the range of RNA amounts that we tested that this was a graded response. It could be that a graded response between transcript abundance and water permeability occurs at lower ratios of PIP1;1 to PIP2;2 than we tested. Alternatively, coexpression may be required in planta to achieve a certain threshold of water permeability, and thereafter posttranslational control may give finer regulation.

We performed in situ hybridization and immunolocalization to determine if *VvPIP1;1* and *VvPIP2;2* genes were expressed in the same cell type, thereby indicating the possibility of interactions between the two proteins. Both genes had similar mRNA expression patterns in Grenache and Chardonnay, particularly in the longitudinal sections at the root tip. This pattern of gene expression for PIPs was similar to that observed in maize longitudinal sections by Hachez et al. (2006). Unfortunately, we were unable to consistently detect *VvPIP1;1* mRNA in the cortical cells at 30 mm from the root tip, but in this tissue it is possible that the presence of large vacuoles effectively reduces signal intensity. Conversely, VvPIP1 protein in particular could be detected in the cortical cells at 30 mm from the root tip. Otto and Kaldenhoff (2000) also detected little tobacco aquaporin *NtAQP1* mRNA in the older parts of the root in contrast to strong protein expression.

Due to the large number of cortical cell layers in grapevine roots, this cell type would likely contribute the greatest quantity of RNA and most likely also account for a large portion of the radial hydraulic resistance. This is supported by the correlation between changes in *VvPIP1;1* expression levels between cultivars and the hydraulic conductivity of cortical cells, which in turn matches with the different diurnal amplitudes that we observed in root L_o between cultivars under water stress. However, we cannot exclude the possibility that endodermal and exodermal cells may have different responses than what we observed in the cortex. The significant increase in *VvPIP1;1* in

Table II. *Accession numbers of aquaporin genes and sequences of primer pairs used for quantitative PCR*

Vitis Gene	Accession No.	Forward/Reverse	Sequence
PIP1;1	EF364432	Forward	5'-AAGAGAAGAGAAGAGAGATGGAAGG-3'
		Reverse	5'-CACATTTCACAGCGTCACCT-3'
PIP1;2	EF364433	Forward	5'-CGCCATCGTCTACAACAAAG-3'
		Reverse	5'-CAGGCTCTGGTCTTGAATGG-3'
PIP1;4	EF364435	Forward	5'-TCTGTTTCTTCTTTTATTTGCTGCT-3'
		Reverse	5'-ATTCAAAAGCTGCCCATTGT-3'
PIP2;1	AY823263	Forward	5'-ACCTTCTCCTGAACCCCCTA-3'
		Reverse	5'-TCATGCCCTCATACATATCAATAAC-3'
PIP2;2	EF364436	Forward	5'-CCACGGTCATAGGCTACAAGAAG-3'
		Reverse	5'-CGAAGGTCACAGCAGGGTTG-3'
PIP2;3	EF364437	Forward	5'-GCCATTGCAGCATTCTATCA-3'
		Reverse	5'-TCCTACAGGGCCACAAATTC-3'
PIP2;4	EF364438	Forward	5'-TTCAGAAGCCTTTTGTACTGGA-3'
		Reverse	5'-GCAGATTGGAAGGCTTTGAC-3'
ACT1	AM465189.1	Forward	5'-GCCTCCGATTCTCTCTGCTCTC-3'
		Reverse	5'-TCACCATTCCAGTTCCATTGTCAC-3'

response to water stress was associated with a significant increase in L_{pcell} of Chardonnay, whereas there was no significant change for Grenache. Increased expression of maize aquaporin $ZmPIP1;2$, an aquaporin that does not transport water, and $ZmPIP2;4$ at 5 to 6 mm compared with 1.5 to 2.5 mm from the root tip was associated with sensitivity of L_{pcell} to a mercury treatment (Hukin et al., 2002). Javot et al. (2003) observed a decrease in L_{pcell} of cortical cells in one line of transgenic Arabidopsis plants with AtPIP2;2 knocked out. This indicated that a single aquaporin isoform made a significant contribution to the hydraulic conductivity of cortical cells, which was associated with a reduction in osmotic hydraulic conductivity of the roots.

In conclusion, the two grapevine cultivars showed contrasting responses to water stress and rewatering. Aquaporins appear to be important contributors to the overall L_o of the root system, as evidenced by the large diurnal change in L_o. These responses were associated with changes in the expression of $VvPIP1;1$. $VvPIP2;2$ appeared to be constitutively expressed in the roots in the situations examined. Even though $VvPIP1;1$ resulted in low water channel activity when expressed in Xenopus oocytes, water permeability increased when $VvPIP1;1$ was coinjected with $VvPIP2;2$. Reduction in root conductance under water stress seems to be constrained in Chardonnay by an increase in the expression of $VvPIP1;1$, resulting in an increased contribution of the cell-to-cell pathway to the radial transport of water during the day. Chardonnay appears to be an "optimistic" cultivar, only reducing L_o in the middle of the day by 2- to 3-fold. This is also consistent with the more anisohydric behavior of this cultivar. The smaller reduction in root hydraulic conductance may also be important in maintaining a small water potential gradient between the xylem and the soil, which could be associated with the lower vulnerability of Chardonnay to embolisms relative to Grenache (Alsina et al., 2007). In contrast, L_o of Grenache was reduced by about 6-fold by water stress in the middle of the day, and there was no up-regulation of $VvPIP1;1$. Grenache had a relatively "pessimistic" response, possibly to restrict water loss to the soil. However, this response would require greater stomatal control in order to prevent excessively negative xylem water potentials. This behavior is consistent with the more isohydric stomatal control in this cultivar (Schultz, 2003). However, Grenache may be able to better respond to rainfall and irrigation events by up-regulation of $VvPIP1;1$.

We have established clear differences in the way roots respond to water stress that correlate with different water use strategies between closely related cultivars of the same species. This indicates that root water transport is closely coupled to shoot transpiration, evident both in the correlation between L_o and transpiration and in the way shoot and root conductances are controlled under different strategies of response to water stress. The challenge now will be to determine the signaling pathways and master switches that coordinate these molecular and anatomical changes within the plant.

MATERIALS AND METHODS

Plant Growth Conditions

One-year-old grapevine (*Vitis vinifera*) rootlings, Chardonnay (clone I10V1) and Grenache (clone BVRC38), were obtained from Yalumba Nursery. Grapevine plants were grown in 20-cm-diameter pots (4.7 L) and repotted into 25-cm pots (9 L) 2 to 3 weeks prior to application of treatments, to prevent the plants from becoming root bound. Grapevine was grown in University of California soil mix: 61.5 L of sand, 38.5 L of peat moss, 50 g of calcium hydroxide, 90 g of calcium carbonate, and 100 g of Nitrophoska (12:5:1, N:P:K plus trace elements) per 100 L at pH 6.8. Pots were placed in a temperature-controlled greenhouse, watered to field capacity every 2 d, and grown over spring and summer. Night/day temperatures were maintained at approximately 19°C/24°C.

Additional grapevine plants were grown in a two-pot system to obtain roots for RNA extraction, in situ hybridization, immunolocalization, root anatomy, and cell pressure probe measurements. The top pot, containing University of California mix, had holes in its base and was covered with plastic netting, and the bottom pot contained a 50:50 mix of vermiculite and perlite that enabled roots to be sampled easily when the top pot was raised. An additional 25 g of Nitrophoska was applied to the top pot approximately every 3 months. Roots were obtained for RNA extraction when the plants were in a growth chamber over winter. Growth chamber temperatures were identical to those in the glasshouse, with a 12-h light period and average light intensity of 200 μmol m^{-2} s^{-1}. The root system hydraulic conductance of the cultivars was not significantly different from that of plants grown in the glasshouse.

Treatments

All treatments were applied in a completely randomized design. Plants were 3 months old, with only vegetative growth that was restricted to two main shoots. Diurnal variability of L_o of Chardonnay was measured every 4 h in a 24-h period, at 6:00 AM, 10:00 AM, 2:00 PM, 6:00 PM, and 10:00 PM. At 6:00 AM and 10:00 PM, the plants were in darkness. In addition, at 6:00 AM and 2:00 PM, L_o was measured on water-stressed plants from which water had been withheld for 8 d. In a separate experiment, well-watered and water-stressed Grenache vines were measured at 6:00 AM and 2:00 PM only.

Chardonnay and Grenache were used to examine the impact of water stress and rewatering on L_o. The two cultivars were examined in separate experiments to prevent diurnal variability affecting the results. Control plants remained well watered, whereas water-stressed plants had water withheld for 8 d. Rewatered plants were stressed for 8 d before watering to field capacity 24 h prior to measurements being taken. Additional well-watered plants were used as controls on the 2nd d with the rewatered plants.

Water Potential

A leaf, eight nodes from the base, was placed in a plastic bag covered with aluminum foil for 1 h prior to measurement in a Scholander pressure chamber (Soil Moisture Equipment Corp.) to determine the Ψ_{stem} (Begg and Turner, 1970). This was performed between 11:00 AM and 1:00 PM and is referred to as midday Ψ_{stem}.

Transpiration

An infrared gas analyzer (type LCA-4 ADC; BioScientific) was used to measure the transpiration of leaves under ambient vapor-pressure deficits at nodes 7, 8, and 9 between 11:00 AM and 12:00 noon before plants were removed for hydraulic conductance measurements. A section of each leaf was placed in the broad leaf chamber while still attached to the plant. Measurements were taken once the substomatal CO_2 concentration had reduced and stabilized.

Hydraulic Conductance

Hydraulic conductance of whole root systems of potted plants was measured with a Dynamax hydraulic conductance flow meter. This is a

destructive technique whereby water is forced to flow into root systems from the cut stump at the base of the shoot and has been shown to give hydraulic conductance values similar to the pressure chamber (Tyree et al., 1995) and the evaporative flux method (Tsuda and Tyree, 1997, 2000). The grapevine stem was cut above the soil surface and covered with filtered (0.22 μm) deionized water, and the stump was connected to the hydraulic conductance flow meter with a water-tight seal. We used the transient ramp technique in the hydraulic conductance flow meter, in which pressure was ramped up to 0.5 MPa at a rate of approximately 7 kPa s^{-1} while simultaneously recording the flow through the roots. On account of the high pressures and the direction of water flow imposed, this technique will not detect changes in hydraulic conductance as the result of xylem embolisms or reduced root-soil contact. There is the possibility that osmotic gradients will be established as solutes are polarized on the inside of the endodermis in the root, because water flows out of the root in the reverse direction to normal flow (Knipfer et al., 2007). It would be predicted that successive application of ramps would polarize solutes further with each ramp because more volume is extruded from the root, which would manifest as a progressive reduction in hydraulic conductance (Figs. 3 and 4; Knipfer et al., 2007). We closely examined both the linearity of each flow versus pressure ramp and the changes that occur from one ramp to the next over three successive ramps done in quick succession for each measurement made under low transpiration (predawn) and high transpiration (midday) conditions. There was no consistent pattern of changes in L_o; successive ramps differed on average by 10.03% $\pm$ 2.37% ($n = 16$). Results were the same for both midday and predawn measurements and did not correlate with the magnitude of hydraulic conductance. The amount of water injected during the ramp was less than 1×10^{-6} m^{-3}, which is small compared with the total estimated volume of the root system of 7×10^{-5} m^{-3}. Generally, an average of the second and third determinations was taken for calculation of L_o, as the slope of the plot of the water flow versus pressure. This was normalized by dividing the conductance by the total root dry weight. For both cultivars, there was a linear correlation between root dry weight and root surface area (which was more difficult to obtain in routine measurements). Measurements were undertaken in the laboratory at a temperature of approximately 21°C to 22°C. The soil was washed from the roots before drying at 60°C for more than 48 h.

Cell Hydraulic Conductivity

A cell pressure probe was used to measure turgor pressure (P), cell elastic volumetric modulus (ε), and half-times of pressure relaxation ($T_{1/2}$) to determine the L_{pcell} (Tyerman et al., 1989; Steudle, 1993). Two to four cells from roots of at least four different plants were measured for each treatment, well watered and water stressed. Water stress was applied for 10 d to obtain midday Ψ_{stem} values similar to those observed in hydraulic conductance experiments. A 40-mm piece of excised root that included the root tip was firmly held in a perspex holder. The roots used were 0.7 to 0.9 mm in diameter and obtained from the two-pot system. A peristaltic pump was used to pump a 1 mM CaSO$_4$ solution around the root at a constant flow rate. Roots were in position for approximately 10 min before measurements commenced, and roots were discarded approximately 1.5 h later. There was no indication of time-dependent changes in turgor pressure after harvesting the roots and bathing them in 1 mM CaSO$_4$ for periods up to 1.5 h.

Microcapillaries were made from borosilicate glass with 1 mm o.d. × 0.58 mm i.d. (GC 100-15 Harvard Apparatus; SDR Clinical Technology). Capillaries were filled with silicone oil and attached to the cell pressure probe with nitrile rubber seals. Roots were probed between 25 and 30 mm from the root tip, and when punctured, cell sap formed a meniscus with the oil.

L_{pcell} was determined using hydrostatic pressure relaxation. Pressure was altered by less than 0.05 MPa via a metal rod (attached to an electric motor) that moved the meniscus to a new position, where it was held in place with small movements of the rod until the pressure equilibrated. Single exponential curves were fitted to pressure relaxations to obtain the $T_{1/2}$ for the rate of water exchange across the cell membrane.

The ε ($\varepsilon = V\Delta P/\Delta V$) was measured by changing cell volumes (ΔV), which caused changes in cell turgor (ΔP). The meniscus was quickly moved and then returned to its original position. L_{pcell} was calculated as $L_{pcell} = V\ln(2)/AT_{1/2}(\varepsilon + \pi_i)$, where V is the cell volume, A is the cell surface area, and π_i is the cell osmotic pressure estimated from steady-state turgor pressure in a solution of known osmotic pressure. SE was determined from the SE values of cell sizes, ε, and $T_{1/2}$ using the differential equation of Gauss for the calculation of error propagation. Unpaired t tests were performed to determine statistical differences between the well-watered and water-stressed cells of Grenache and Chardonnay for the parameters measured.

Root Anatomy

Roots were sampled from the two-pot system from well-watered and water-stressed plants. Water stress was applied for 10 d to obtain midday Ψ_{stem} values similar to those observed in hydraulic conductance experiments. Free-hand cross sections were taken at 25 and 50 mm from the root tip using a total of six roots from at least three different plants. Suberin lamellae were detected by staining for 2 h with 0.1% (w/v) Sudan Red 7B (Sigma) and then mounting in 75% (v/v) glycerol (Brundrett et al., 1991). Bright-field images were taken with a Zeiss Aixophot Pol Photomicroscope.

RNA Extraction

Grapevine plants were grown in a two-pot system, and the apical 50 mm of the roots from the bottom pot was carefully and quickly harvested, frozen in liquid nitrogen, and stored at −70°C. Replicate RNA samples were prepared from 350 mg of roots from three different plants per treatment. Roots were harvested every 4 h at 6:00 AM, 10:00 AM, 2:00 PM, 6:00 PM, and 10:00 PM from well-watered Chardonnay vines. In two separate experiments, roots were harvested from Grenache and Chardonnay vines that had been well watered, water stressed for 10 d, or water stressed for 10 d and then rewatered 24 h prior to harvest. Water stress was applied for 10 d to obtain midday Ψ_{stem} values similar to those observed in hydraulic conductance experiments.

RNA was extracted with 5 M sodium perchlorate, 0.2 M Tris, pH 8.3, 8.5% (w/v) polyvinylpolypyrrolidone, 5% (w/v) SDS, and 1% (v/v) β-mercaptoethanol for 30 min at room temperature. Samples were then processed with a modified protocol of the RNeasy Plant Mini Kit (Qiagen; Franks et al., 2006). Contaminating DNA was removed with Turbo DNase treatment for 20 min at 37°C (Ambion), and RNA was stored at −70°C. Total RNA was quantified with a UV spectrophotometer. The presence of contamination from genomic DNA was tested for by reverse transcription (RT)-PCR.

Quantitative PCR

Primers for quantitative PCR were designed based on published sequences of aquaporins found in grapevine (Table II), with the criteria of a melting temperature of 59°C $\pm$ 1°C, primer length of 20 to 24 bp, a product size of 110 to 150 bp, and a GC content of 45% to 60%. To create stock solutions for each PCR product, individual RT-PCRs were performed on total RNA extracted from well-watered Chardonnay roots. Amplified cDNAs were separated on a 1.5% agarose gel, and correctly sized bands were excised and then eluted with the MinElute Gel Extraction Kit (Qiagen). This stock solution was used to create a dilution series covering 5 orders of magnitude ($x \times 10^{-3}$–10^{-7}). Two replicates of each of the five standard concentrations were included with every quantitative PCR experiment, together with no-template controls. For $VvPIP1;1$, $VvPIP2;2$, and $VvACT1$ (reference gene), the concentration of each cDNA stock solution was determined using fluorescent PicoGreen reagent (Invitrogen), with excitation at 480 nm and emission at 520 nm, using a VersaFluor fluorometer (Bio-Rad) against a known DNA standard (Invitrogen).

For each RNA sample, 1 μg was reverse transcribed using the iScript cDNA synthesis kit (Bio-Rad). The thermocycler was programmed for one cycle of 5 min at 25°C, 30 min at 42°C, and 5 min at 85°C. Quantitative PCR was performed with an iCycler (Bio-Rad) in a reaction volume of 20 μL containing 10 μL of SBYR Green Mix (Bio-Rad), 0.6 μM primer, and 1 μL of cDNA. The PCR cycle profile was as follows: one cycle of 2 min at 95°C, and 40 cycles of 30 s at 95°C, 30 s at 57°C, and 15 s at 72°C. Amplification data were collected during the extension step (72°C). Melt curve analyses were made by elevating the temperature from 55°C to 99°C at a rate of 0.5°C s^{-1}. Only a single band with a characteristic melting point was observed for each sample, indicating that the product was specific to the primers. Products were routinely checked by 1.5% (w/v) agarose gel electrophoresis.

To determine the relative gene expression of the eight aquaporins in the root tissue of well-watered Chardonnay, the method described by Muller et al. (2002) was used. In experiments examining diurnal variation and the impact of water stress, only changes in the expression of $VvPIP1;1$ and $VvPIP2;2$ were determined. In these quantitative PCR experiments, standard curves using known amounts of cDNA were used to quantify the starting amounts of cDNA for each gene. The final value of relative gene expression is the ratio of the starting quantity of the gene of interest to the starting quantity of $VvACT1$, the reference gene, to account for differences in the original RNA concentration and the efficiency of cDNA transcription. $VvACT1$ expression was not

significantly different between treatments. For each treatment, there were three biological replicates.

Expression in *Xenopus laevis* Oocytes

The cDNAs of *VvPIP1;1* (accession no. EF364432) and *VvPIP2;2* (accession no. EF364436), obtained by RT-PCR, were cloned into the expression vector pGEMHE using the restriction enzymes *Bst*EII for *VvPIP1;1* and *Pvu*II for *VvPIP2;2*. pGEMHE carries the 5′ and 3′ untranslated sequences of the β-globin gene from *X. laevis* in order to promote the translation efficiency of plant cRNA (Linman et al., 1992). The positive control, *HsAQP1* (accession no. P29972), was cloned into the vector pXBG using the restriction enzyme *Bgl*II. Capped cRNAs were synthesized from plasmids linearized with *Nhe*I for grapevine aquaporins and *Sma*I for AQP1 using the mCAP RNA capping kit (Stratagene). *X. laevis* oocytes were isolated and digested at room temperature for 70 min with 2 mg mL^{-1} collagenase in ND96 (96 mM NaCl, 1 mM KCl, 1 mM MgCl$_2$, and 5 mM HEPES-NaOH, pH 7.5). Oocytes were defolliculated with a hypotonic buffer (100 mM KH$_2$PO$_4$-KOH and 0.1% BSA, pH 6.5) and washed twice in ND96 and then with Ca-free Ringer's solution (96 mM NaCl, 2 mM KCl, 5 mM MgCl$_2$, and 5 mM HEPES-NaOH, pH 7.6). Prepared oocytes were stored in Ca-Ringer's solution (Ca-free Ringer's solution + 0.6 mM CaCl$_2$) supplemented with horse serum (5%; Sigma Chemical Company) and antibiotics (100 units mL^{-1} penicillin, 0.1 mg mL^{-1} streptomycin, and 0.05 mg mL^{-1} tetracycline) prior to injection (Nanoject II microinjector; Drummond Scientific Company) with cRNA or sterile diethyl pyrocarbonate-treated water in a volume of 46 nL. The capillaries used were pulled in two stages with a capillary puller on heat settings 11.83 and 9 (Narishige Scientific Equipment Laboratory). There was 12 ng of either *VvPIP1;1* or *VvPIP2;2* injected or 12 ng of each injected together to create a 1:1 ratio. To create the 0.5:1, 2:1, and 3:1 ratios of *VvPIP1;1*:*VvPIP2;2*, the amount of *VvPIP2;2* remained at 12 ng with the amount of *VvPIP1;1* adjusted accordingly. After injection, oocytes were incubated in Ca-Ringer's solution plus horse serum and antibiotics (as above) for 3 d at 18°C. The P_{os} was determined by transferring the oocytes to the same solution diluted 5-fold (from 215 to 43 mosmol), and the changes in volume were captured with a Vicam color camera (Pacific Communications) attached to a Nikon SMZ800 microscope. Images were analyzed using the computer program Global Lab Image-2 (Data Translation) using the Blob Analysis Tool to determine the change in the total area of the oocytes captured in the AVI video file. The change in area was used to calculate the change in volume assuming that the oocytes were spheres. The P_{os} was determined from the initial rate of change of relative cell volume [$J_w = d(V/V_o)/dt$] using the equation $P_{os} = J_w/V_w \times A \times \Delta Osm$, where A = area of oocyte, ΔOsm = change in osmolarity, and V_w = partial molar volume of water (18 mL mol^{-1}).

In Situ Hybridization

Digoxigenin-labeled antisense and sense *VvPIP1;1* and *VvPIP2;2* probes were generated with the DIG RNA labeling kit as described by the manufacturer (Roche Diagnostics) using template synthesized by in vitro transcription of PCR products with a T7 promoter sequence upstream (antisense) or downstream (sense) for each of the *VvPIP1;1* and *VvPIP2;2* fragments. Probes of 176 and 180 bp (*VvPIP1;1* and *VvPIP2;2*, respectively) were designed to target 3′ untranslated regions specific to each gene

Grenache and Chardonnay roots, sampled at the root tip and 30 and 50 mm from the tip, were fixed for 2 h in FAA (50% ethanol, 5% acetic acid, 4% formaldehyde, 0.1% Tween 20) and processed as described by Sutton et al. (2007) with the following modifications. Probes were hybridized at final concentrations of 0.5 and 1 ng nL^{-1} for *VvPIP2;2* and *VvPIP1;1*, respectively, in hybridization buffer (50% formamide, 2× SSC, 10% dextran sulfate, 1× Denhardt's solution, and 1 μg μL^{-1} tRNA). In situ hybridization was performed overnight at 50°C and 45°C for *VvPIP2;2* and *VvPIP1;1*, respectively, and washes were in 0.2× SSC at the corresponding temperatures. In addition to sense probe controls, controls were made with no probe. Images were taken with a Leica AS LMD microscope. *VvPIP2;2* longitudinal images were taken after 3 h of development, with the remaining images taken at 24 h.

Immunolocalization

Custom-designed KLH peptide-conjugated oligonucleotide sequences were synthesized and injected into New Zealand White rabbits to produce antibodies against all known plant PIP1s and all known PIP2s in grapevine

(Sigma-Genosys). For VvPIP1, we used an N-terminal sequence (5′-GKE-EDVRLGANKFPERQPIGSTAQ-3′), and for VvPIP2, we used a C-terminal sequence (5′-CRAGAIKALGSFRS-3′).

Grenache and Chardonnay roots were sampled at the root tip and at 30 and 50 mm from the tip, fixed for 2 h in TEM fixative (0.25% glutaraldehyde, 4% paraformaldehyde, and 4% Suc in 1× phosphate-buffered saline), and processed, embedded, and sectioned as described previously (Sutton et al., 2007). Sections were dewaxed twice for 10 min each in xylene and rehydrated through an ethanol series into phosphate-buffered saline, pH 7.4, then blocked for 30 min in 1% (w/v) bovine serum albumin in phosphate-buffered saline. Primary antibody was applied for 1 h at room temperature, slides were washed three times in blocking buffer, secondary antibody (Alexa Fluor 568 goat anti-rabbit IgG [H+L]; Molecular Probes) was applied for 1.5 h, and slides were washed three times in blocking buffer and then mounted in 90% glycerol:10% water (v/v). Controls were made with no primary and/or no secondary antibody. Images were taken with a Leica AS LMD microscope equipped with fluorescence filter N2.1 (excitation filter, 515–560 nm BP; barrier filter, 590 LP), with exposure standardized at 9 s.

Statistical Analysis

Statistical analysis was performed using the statistics package Genstat version 6 (Numerical Algorithms Group). Differences were accepted as significant at $P < 0.05$.

ACKNOWLEDGMENTS

LITERATURE CITED

Aharon R, Shahak Y, Wininger S, Bendov R, Kapulnik Y, Galili G (2003) Overexpression of a plasma membrane aquaporin in transgenic tobacco improves plant vigor under favorable growth conditions but not under drought or salt stress. Plant Cell **15**: 439–447

Alexandersson E, Fraysse L, Sjovall-Larsen S, Gustavsson S, Fellert M, Karlsson M, Johanson U, Kjellbom P (2005) Whole gene family expression and drought stress regulation of aquaporins. Plant Mol Biol **59**: 469–484

Alleva K, Niemietz CM, Maurel C, Parisi M, Tyerman SD, Amodeo G (2006) Plasma membrane of *Beta vulgaris* storage root shows high water channel activity regulated by cytoplasmic pH and a dual range of calcium concentrations. J Exp Bot **57**: 609–621

Alsina MM, de Herralde F, Aranda X, Save R, Biel C (2007) Water relations and vulnerability to embolism are not related: experiments with eight grapevine cultivars. Vitis **46**: 1–6

Aroca R, Ferrante A, Vernieri P, Chrispeels MJ (2006) Drought, abscisic acid and transpiration rate effects on the regulation of PIP aquaporin gene expression and abundance in *Phaseolus vulgaris* plants. Ann Bot (Lond) **98**: 1301–1310

Begg JE, Turner NC (1970) Water potential gradients in field tobacco. Plant Physiol **46**: 343–346

Bramley H, Turner DW, Tyerman SD, Turner NC (2007a) Water flow in the roots of crop species: the influence of root structure, aquaporin activity, and water logging. Adv Agron **96**: 133–196

Bramley H, Turner NC, Turner DW, Tyerman SD (2007b) Comparison between gradient-dependent hydraulic conductivities of roots using the root pressure probe: the role of pressure propagations and implications for the relative roles of parallel radial pathways. Plant Cell Environ **30**: 861–874

Brundrett MC, Kendrick B, Peterson CA (1991) Efficient lipid staining in

plant material with Sudan red-7B or fluorol yellow-088 in polyethylene glycol-glycerol. Biotech Histochem 66: 111–116

Chaumont F, Barrieu F, Jung R, Chrispeels MJ (2000) Plasma membrane intrinsic proteins from maize cluster in two sequence subgroups with differential aquaporin activity. Plant Physiol 122: 1025–1034

Cruz RT, Jordan WR, Drew MC (1992) Structural changes and associated reduction of hydraulic conductance in roots of *Sorghum bicolor* L. following exposure to water deficit. Plant Physiol 99: 203–212

Cui XH, Hao FS, Chen H, Chen J, Wang XC (2008) Expression of the *Vicia faba VfPIP1* gene in *Arabidopsis thaliana* plants improves their drought resistance. J Plant Res 121: 207–214

DeBolt S, Cook DR, Ford CM (2006) L-Tartaric acid synthesis from vitamin C in higher plants. Proc Natl Acad Sci USA 103: 5608–5613

Dry PR, Loveys BR (1998) Factors influencing grapevine vigour and the potential for control with partial rootzone drying. Aust J Grape Wine Res 4: 140–148

Düring H, Dry PR (1995) Osmoregulation in water-stressed roots: responses of leaf conductance and photosynthesis. Vitis 34: 15–17

Fan L, Linker R, Gepstein S, Tanimoto E, Yamamoto R, Neumann PM (2006) Progressive inhibition by water deficit of cell wall extensibility and growth along the elongation zone of maize roots is related to increased lignin metabolism and progressive stelar accumulation of wall phenolics. Plant Physiol 140: 603–612

Fetter K, Van Wilder V, Moshelion M, Chaumont F (2004) Interactions between plasma membrane aquaporins modulate their water channel activity. Plant Cell 16: 215–228

Fouquet R, Léon C, Ollat N, Barrieu F (2008) Identification of grapevine aquaporins and expression analysis in developing berries. Plant Cell Rep 27: 1541–1550

Franks PJ, Drake PL, Froend RH (2007) Anisohydric but isohydrodynamic: seasonally constant plant water potential gradient explained by a stomatal control mechanism incorporating plant hydraulic conductance. Plant Cell Environ 30: 19–30

Franks TK, Powell KS, Choimes S, Marsh E, Iocco P, Sinclair BJ, Ford CM, van Heeswijck R (2006) Consequences of transferring three sorghum genes for secondary metabolite (cyanogenic glucoside) biosynthesis to grapevine hairy roots. Transgenic Res 15: 181–195

Galmés J, Pou A, Alsina MM, Tomàs M, Medrano H, Flexas J (2007) Aquaporin expression in response to different water stress intensities and recovery in Richter-110 (*Vitis* sp.): relationship with ecophysiological status. Planta 226: 671–681

Gerbeau P, Amodeo G, Henzler T, Santoni V, Ripoche P, Maurel C (2002) The water permeability of *Arabidopsis* plasma membrane is regulated by divalent cations and pH. Plant J 30: 71–81

Gibberd MR, Walker RR, Blackmore DH, Condon AG (2001) Transpiration efficiency and carbon-isotope discrimination of grapevines grown under well-watered conditions in either glasshouse or vineyard. Aust J Grape Wine Res 7: 110–117

Hachez C, Moshelion M, Zelazny E, Cavez D, Chaumont F (2006) Localization and quantification of plasma membrane aquaporin expression in maize primary root: a clue to understanding their role as cellular plumbers. Plant Mol Biol 62: 305–323

Henzler T, Waterhouse RN, Smyth AJ, Carvajal M, Cooke DT, Schäffner AR, Steudle E, Clarkson DT (1999) Diurnal variations in hydraulic conductivity and root pressure can be correlated with the expression of putative aquaporins in the roots of *Lotus japonicus*. Planta 210: 50–60

Hukin D, Doering Saad C, Thomas CR, Pritchard J (2002) Sensitivity of cell hydraulic conductivity to mercury is coincident with symplasmic isolation and expression of plasmalemma aquaporin genes in growing maize roots. Planta 215: 1047–1056

Jaillon O, Aury JM, Noel B, Policriti A, Clepet C, Casagrande A, Choisne N, Aubourg S, Vitulo N, Jubin C, et al (2007) The grapevine genome sequence suggests ancestral hexaploidization in major angiosperm phyla. Nature 449: 463–467

Jang JY, Kim DG, Kim YO, Kim JS, Kang HS (2004) An expression analysis of a gene family encoding plasma membrane aquaporins in response to abiotic stresses in *Arabidopsis thaliana*. Plant Mol Biol 54: 713–725

Javot H, Lauvergeat V, Santoni V, Martin-Laurent F, Guclu J, Vinh J, Heyes J, Franck KI, Schaffner AR, Bouchez D, et al (2003) Role of a single aquaporin isoform in root water uptake. Plant Cell 15: 509–522

Johanson U, Karlsson M, Johansson I, Gustavsson S, Sjovall S, Fraysse L, Weig AR, Kjellbom P (2001) The complete set of genes encoding major intrinsic proteins in Arabidopsis provides a framework for a new nomenclature for major intrinsic proteins in plants. Plant Physiol 126: 1358–1369

Johansson I, Karlsson M, Shukla VK, Chrispeels MJ, Larsson C, Kjellbom P (1998) Water transport activity of the plasma membrane aquaporin PM28A is regulated by phosphorylation. Plant Cell 10: 451–459

Knipfer T, Das D, Steudle E (2007) During measurements of root hydraulics with pressure probes, the contribution of unstirred layers is minimized in the pressure relaxation mode: comparison with pressure clamp and high-pressure flowmeter. Plant Cell Environ 30: 845–860

Linman ER, Tytgat J, Hess P (1992) Subunit stoichiometry of a mammalian K1 channel determined by construction of multimeric cDNAs. Neuron 9: 861–871

Lo Gullo MA, Nardini A, Salleo S, Tyree MT (1998) Changes in root hydraulic conductance (K_r) of *Olea oleaster* seedlings following drought stress and irrigation. New Phytol 140: 25–31

Lopez M, Bousser AS, Sissoeff I, Gaspar M, Lachaise B, Hoarau J, Mahe A (2003) Diurnal regulation of water transport and aquaporin gene expression in maize roots: Contribution of PIP2 proteins. Plant Cell Physiol 44: 1384–1395

Mariaux JB, Bockel C, Salamini F, Bartels D (1998) Desiccation- and abscisic acid-responsive genes encoding major intrinsic proteins (MIPs) from the resurrection plant *Craterostigma plantagineum*. Plant Mol Biol 38: 1089–1099

Martre P, Morillon R, Barrieu F, North GB, Nobel PS, Chrispeels MJ (2002) Plasma membrane aquaporins play a significant role during recovery from water deficit. Plant Physiol 130: 2101–2110

Martre P, North GB, Nobel PS (2001) Hydraulic conductance and mercury-sensitive water transport for roots of *Opuntia acanthocarpa* in relation to soil drying and rewetting. Plant Physiol 126: 352–362

Maurel C, Kado RT, Guern J, Chrispeels MJ (1995) Phosphorylation regulates the water channel activity of the seed-specific aquaporin α-TIP. EMBO J 14: 3028–3035

McElrone AJ, Bichler J, Pockman WT, Addington RN, Linder CR, Jackson RB (2007) Aquaporin-mediated changes in hydraulic conductivity of deep tree roots accessed via caves. Plant Cell Environ 30: 1411–1421

Meinzer FC, Grantz DA (1990) Stomatal and hydraulic conductance in growing sugarcane: stomatal adjustment to water transport capacity. Plant Cell Environ 13: 383–388

Moshelion M, Becker D, Biela A, Uehlein N, Hedrich R, Otto B, Levi H, Moran N, Kaldenhoff R (2002) Plasma membrane aquaporins in the motor cells of *Samanea saman*: diurnal and circadian regulation. Plant Cell 14: 727–739

Muller PY, Janovjak H, Miserez AR, Dobbie Z (2002) Processing of gene expression data generated by quantitative real-time RT-PCR. Biotechniques 32: 1372–1379

North GB, Nobel PS (1991) Changes in hydraulic conductivity and anatomy caused by drying and rewetting roots of *Agave deserti* (Agavaceae). Am J Bot 78: 906–915

North GB, Martre P, Nobel PS (2004) Aquaporins account for variations in hydraulic conductance for metabolically active root regions of *Agave deserti* in wet, dry and rewetted soil. Plant Cell Environ 27: 219–228

North GB, Nobel PS (1995) Hydraulic conductivity of concentric root tissues of *Agave deserti* Engelm under wet and drying conditions. New Phytol 130: 47–57

North GB, Nobel PS (1996) Radial hydraulic conductivity of individual root tissues of *Pountia ficus-indica* (L.) Miller as soil moisture varies. Ann Bot (Lond) 77: 133–142

North GB, Nobel PS (2000) Heterogeneity in water availability alters cellular development and hydraulic conductivity along roots of a desert succulent. Ann Bot (Lond) 85: 247–255

Otto B, Kaldenhoff R (2000) Cell-specific expression of the mercury-insensitive plasma-membrane aquaporin NtAQP1 from *Nicotiana tabacum*. Planta 211: 167–172

Saliendra NZ, Sperry JS, Comstock JP (1995) Influence of leaf water status on stomatal response to humidity, hydraulic conductance and soil drought in *Betula occidentalis*. Planta 196: 357–366

Sarda X, Tousch D, Ferrare K, Cellier F, Alcon C, Dupuis JM, Casse F, Lamaze T (1999) Characterization of closely related δ-TIP genes encoding aquaporins which are differentially expressed in sunflower roots upon water deprivation through exposure to air. Plant Mol Biol 40: 179–191

Schäffner AR (1998) Aquaporin function, structure, and expression: are there more surprises to surface in water relations? Planta 204: 131–139

Schultz HR (2003) Differences in hydraulic architecture account for near

isohydric and anisohydric behaviours of two field-grown *Vitis vinifera* L. cultivars during drought. Plant Cell Environ 26: 1393–1405

Secchi F, Lovisolo C, Uehlein N, Kaldenhoff R, Schubert A (2007) Isolation and functional characterization of three aquaporins from olive (*Olea europaea* L.). Planta 225: 381–392

Sharp RE, Hsiao TC, Silk WK (1990) Growth of the maize primary root at low water potentials. 2. Role of growth and deposition of hexose and potassium in osmotic adjustment. Plant Physiol 93: 1337–1346

Sharp RE, Poroyko V, Hejlek LG, Spollen WG, Springer GK, Bohnert HJ, Nguyen HT (2004) Root growth maintenance during water deficits: physiology to functional genomics. J Exp Bot 55: 2343–2351

Shelden MC (2007) A comparison of water stress-induced xylem embolism in two grapevine cultivars, Chardonnay and Grenache, and the role of aquaporins. PhD thesis. University of Adelaide, Adelaide, Australia

Siefritz F, Tyree MT, Lovisolo C, Schubert A, Kaldenhoff R (2002) PIP1 plasma membrane aquaporins in tobacco: from cellular effects to function in plants. Plant Cell 14: 869–876

Siemens JA, Zwiazek JJ (2003) Effects of water deficit stress and recovery on the root water relations of trembling aspen (*Populus tremuloides*) seedlings. Plant Sci 165: 113–120

Soar CJ, Speirs J, Maffei SM, Penrose AB, McCarthy MG, Loveys BR (2006) Grape vine varieties Shiraz and Grenache differ in their stomatal response to VPD: apparent links with ABA physiology and gene expression in leaf tissue. Aust J Grape Wine Res 12: 2–12

Sommer A, Geist B, Da Ines O, Gehwolf R, Schäffner AR, Obermeyer G (2008) Ectopic expression of *Arabidopsis thaliana* plasma membrane intrinsic protein 2 aquaporins in lily pollen increases the plasma membrane water permeability of grain but not of tube protoplasts. New Phytol 180: 787–797

Sperry JS, Alder NN, Eastlack SE (1993) The effect of reduced hydraulic conductance on stomatal conductance and xylem cavitation. J Exp Bot 44: 1075–1082

Steudle E (1993) Pressure probe techniques: basic principles and application of studies of water and solute relations at the cell, tissue and organ level. *In* JAC Smith, H Griffiths, eds, Water Deficits: Plant Responses from Cell to Community. BIOS Scientific Publishers, Oxford, pp 5–36

Steudle E (2000a) Water uptake by roots: effects of water deficit. J Exp Bot 51: 1531–1542

Steudle E (2000b) Water uptake by plant roots: an integration of views. Plant Soil 226: 45–56

Steudle E, Heydt H (1997) Water transport across tree roots. *In* H Rennenberg, W Eschrich, H Ziegler, eds, Trees: Contributions to Modern Tree Physiology: Backhuys Publishers, Leiden, The Netherlands, pp 239–255

Steudle E, Peterson CA (1998) How does water get through roots? J Exp Bot 49: 775–788

Suga S, Komatsu S, Maeshima M (2002) Aquaporin isoforms responsive to salt and water stresses and phytohormones in radish seedlings. Plant Cell Physiol 43: 1229–1237

Sutton T, Baumann U, Hayes J, Collins NC, Shi BJ, Schnurbusch T, Hay A, Mayo G, Pallotta M, Tester M, et al (2007) Boron toxicity tolerance in barley arising from efflux transporter amplification. Science 318: 1446–1449

Temmei Y, Uchida S, Hoshino D, Kanzawa N, Kuwahara M, Sasaki S, Tsuchiya T (2005) Water channel activities of *Mimosa pudica* plasma membrane intrinsic proteins are regulated by direct interaction and phosphorylation. FEBS Lett 579: 4417–4422

Tilbrook J, Tyerman SD (2008) Cell death in grape berries: varietal differences linked to xylem pressure and berry weight loss. Funct Plant Biol 35: 173–184

Tournaire-Roux C, Sutka M, Javot H, Gout E, Gerbeau P, Luu DT, Bligny R, Maurel C (2003) Cytosolic pH regulates root water transport during anoxic stress through gating of aquaporins. Nature 425: 393–397

Troggio M, Vezzulli S, Pindo M, Malacarne G, Fontana P, Moreira FM, Costantini L, Grando MS, Viola R, Velasco R (2008) Beyond the genome, opportunities for a modern viticulture: a research overview. Am J Enol Vitic 59: 117–127

Tsuda M, Tyree MT (1997) Whole-plant hydraulic resistance and vulnerability segmentation in *Acer saccharinum*. Tree Physiol 17: 351–357

Tsuda M, Tyree MT (2000) Plant hydraulic conductance measured by the high pressure flow meter in crop plants. J Exp Bot 51: 823–828

Tyerman SD, Niemietz CM, Bramley H (2002) Plant aquaporins: multifunctional water and solute channels with expanding roles. Plant Cell Environ 125: 173–194

Tyerman SD, Oats P, Gibbs J, Dracup M, Greenway H (1989) Turgor regulation and cellular water relations of *Nicotiana tabacum* roots grown in high salinities. Aust J Plant Physiol 16: 517–531

Tyree MT, Patino S, Bennink J, Alexander J (1995) Dynamic measurements of root hydraulic conductance using a high-pressure flowmeter in the laboratory and field. J Exp Bot 46: 83–94

Vandeleur R, Niemetz C, Tilbrook J, Tyerman SD (2005) Roles of aquaporins in root responses to irrigation. Plant Soil 274: 141–161

Voetberg GS, Sharp RE (1991) Growth of the maize primary root at low water potentials. 3. Role of increased proline deposition in osmotic adjustment. Plant Physiol 96: 1125–1130

Wan X, Steudle E, Hartung W (2004) Gating of water channels (aquaporins) in cortical cells of young corn roots by mechanical stimuli (pressure pulses): effects of ABA and HgCl₂. J Exp Bot 55: 411–422

Wu Y, Sharp RE, Durachko DM, Cosgrove DJ (1996) Growth maintenance of the maize primary root at low water potentials involves increases in cell-wall extension properties, expansin activity, and wall susceptibility to expansins. Plant Physiol 111: 765–772

Yamada S, Komori T, Myers PN, Kuwata S, Kubo T, Imaseki H (1997) Expression of plasma membrane water channel genes under water stress in *Nicotiana excelsior*. Plant Cell Physiol 38: 1226–1231

Ye Q, Wiera B, Steudle E (2004) A cohesion/tension mechanism explains the gating of water channels (aquaporins) in *Chara* internodes by high concentration. J Exp Bot 55: 449–461

Yu Q, Hu Y, Li J, Wu Q, Zhongping L (2005) Sense and antisense expression of plasma membrane aquaporin *BnPIP1* from *Brassicus napus* in tobacco and its effects on plant drought resistance. Plant Sci 168: 647–656

Zelazny E, Borst JW, Muylaert M, Batoko H, Hemminga MA, Chaumont F (2007) FRET imaging in living maize cells reveals that plasma membrane aquaporins interact to regulate their subcellular localization. Proc Natl Acad Sci USA 104: 12359–12364

Zhou Y, Setz N, Niemietz C, Qu H, Offler CE, Tyerman SD, Patrick JW (2007) Aquaporins and unloading of phloem-imported water in coats of developing bean seeds. Plant Cell Environ 30: 1566–1577